1 Title: Avian telencephalon and cerebellum volumes can be accurately estimated from digital brain
2 endocasts

3 Aubrey R. Keirnan[1], Felipe Cunha[2], Sara Citron[2], Gavin Prideaux[1], Andrew N. Iwaniuk[2]*, Vera
4 Weisbecker[1]*
5
6 [1] College of Science and Engineering, Flinders University, Adelaide SA, Australia
7 [2] Department of Neuroscience, University of Lethbridge, Lethbridge, Alberta, Canada
8 ORCiD:
9 Aubrey Keirnan 0000-0002-4033-6217
10 Felipe Cunha 0000-0002-3656-732X
11 Sara Citron 0009-0006-8138-3905
12 Gavin Prideaux 0000-0002-9958-0265
13 Andrew N. Iwaniuk 0000-0001-9273-3655
14 Vera Weisbecker 0000-0003-2370-4046

ABSTRACT

For studies of the evolution of vertebrate brain anatomy and potentially associated behaviours, reconstructions of digital brain endocasts from computed tomography scans have revolutionised our capacity to collect neuroanatomical data. However, measurements from digital endocasts must be validated as reflecting actual brain anatomy, which is difficult because the collection of soft tissue information through histology is laborious and time consuming. In birds, the reliability of digital endocast measurements as volume proxies for the two largest brain regions – the telencephalon and cerebellum - remains to be validated despite their use as proxies e.g. of cognitive performance or flight ability. We here use the largest dataset of histology and digital endocasts to date, including 136 species from 25 avian orders, to compare digital endocast surface area measurements with actual brain volumes of the telencephalon, cerebellum, and whole-brain endocast. Using linear and phylogenetically informed regression analyses, we demonstrate that endocast surfaces are strongly correlated with their brain volume counterparts for both absolute and relative size. This provides empirical support for using endocast-derived cerebellar and telencephalic surface areas in existing and future studies of living and extinct birds, with potential to expand to the dinosaur-bird transition in the future.

INTRODUCTION

Over the past two decades, digital endocasts have become an increasingly important tool in the study of neural and behavioural evolution in vertebrates [1-6]. Using computed tomography (CT) scanned skulls, the brain cavity is digitally "filled" to approximate the volume and shape of the brain [7]. These methods are largely non-destructive, allowing research into the neuroanatomy of rare [8] and extinct species [9], including fossil specimens [10, 11]. For preservation purposes, such as museum specimens or fossils embedded in sedimentary matrix, CT scanning offers non-destructive access to otherwise unattainable information [12, 13]. To date, endocasts have been used to study brain evolution across all vertebrate classes, including fishes [5], amphibians [2], birds [14], non-avian reptiles [15, 16], and mammals [6, 17, 18]. Therefore, our understanding of the brain-to-endocast relationship is fundamental to the study of vertebrate brain evolution.

Our knowledge of evolutionary patterns in brain size [13, 19], shape [6, 20], and composition [21] has advanced substantially over the past century through endocast comparisons [13, 22]. For example, early endocast research on pterosaur fossils, an extinct clade of flying reptiles, revealed similarities between their brains with those of modern birds [23]. These included the positions of the optic lobes (or midbrain) and the cerebellum, distinguishing pterosaurs and birds from other reptiles [23]. More recently, endocast studies have been used to infer brain–behaviour relationships, including social behaviour in big cats [24], nocturnality in birds [8, 9, 25], and the habitats of snakes [16]. However, there is substantial variation in the brain–endocast relationships among vertebrates [26], yet the use of endocast measurements relies on the assumption that they are indicative of the brain region of interest [2, 3, 12]. While some studies have verified the brain–endocast correlations for particular brain regions [27, 28], measurement modalities such as shape or volume are not necessarily interchangeable [4, 6], meaning that both must be tested to establish the validity of these methods. For fishes, amphibians, and non-avian reptiles, in which brains do not fill the cranial cavity, inferences are limited as endocasts

overestimate brain size [2, 4, 29]. This can be an issue particularly at the root of iconic radiations such as dinosaurs, whose closest living non-avian relatives – the crocodiles – have brains that typically occupy less than half of their endocranial space in adults [26, 30]. In contrast, the endocranial volume in birds is strongly correlated with brain volume [31].

The brains of birds have been the subject of extensive efforts to establish the relationship between the endocranial cavity and brain tissue [22, 28, 31-33]. Their endocasts are remarkably faithful to the shape of the brain itself, and endocranial volume is a valid proxy for actual brain volume and widely used in studies of brain size (e.g. [14, 31, 34, 35]). Further, several brain regions are discernible in endocasts [10, 12, 22, 28]. The endocast surface areas of two of these brain regions, the wulst and optic lobes, are reliable estimates of the underlying hyperpallium and optic tectum regions, respectively, of the brain [28]. However, inferences have also been drawn from endocast measurements of the telencephalon and cerebellum, even though the reliability of measuring these brain regions from endocasts remains untested. Changes in the size of both regions are important in the evolution of differences in avian cognition [36] and the brain becoming “flight-ready” [37, 38]. For example, the expansion of the telencephalon is a key anatomical change in the evolution of the avian brain [37, 39] and associated with higher rates of innovative behaviour [40]. Similarly, changes in relative cerebellum size, and part of the cerebellum, are associated with behavioural differences across avian clades [41, 42]. They also comprise the majority of brain volume [43] and the endocast surface. Exploiting the potential of these two brain regions in explaining major transitions in avian brain evolution therefore requires validation of how faithfully their endocast imprints reflect their soft tissue volume.

Here, we determine the brain–endocast relationships of the telencephalon and cerebellum using the largest, phylogenetically diverse sample of bird species to date. While brain regions are typically measured as volumes, endocasts lack the internal anatomical landmarks needed to accurately divide them into volumes. This is especially true of the avian cerebellum, because its

anterior surface is covered by the posterior telencephalon. While surface area may not be interchangeable with volume [6], we hypothesised this comparison would show a typical isometric relationship, close to or equal to a 2:3 ratio or surface area increasing at a rate of 0.67 to that of the volume. However, as the relative size of these brain regions is often important for studying neurobehavioural evolution [3, 26, 32, 44, 45], we also asked if their relative size when measured from endocasts was comparable to that of brains. We expected that, if the endocast reliably estimates the relative size of these regions, they would produce comparable relationships, which would result in similar slopes.

90 **METHODS**

91 *Specimens*

92 Data on whole brain, telencephalon and cerebellum volumes were compiled from the literature [41,
93 43, 46-56] and supplemented with previously unpublished data from a histological collection
94 maintained by ANI [57]. These specimens were provided to ANI dead and were not euthanised for the
95 purpose of this study. Further, all procedures were completed in accordance with the guidelines and
96 policies of the Canada Council on Animal Care. All of these brains were gelatin-embedded and serially
97 sectioned in the coronal plane at a thickness of 40µm. After mounting and staining with thionin
98 acetate, the volumes were measured using unbiased stereology in StereoInvestigator
99 (Microbrightfield Inc., VT, USA) by FC. For some species, the telencephalon and cerebellum volumes
100 were measured from different individuals. In such cases, we included the brain volumes for both
101 individuals to accurately calculate the relative size of brain regions. More details on the brain
102 processing and volume measurement methods are described in [46]. All data and their specific sources
103 are provided in the electronic supplementary material [58].

104 To compare the brain volumes with surface areas from endocasts, we collected existing micro-
105 computed tomography (µCT) scans as well as completing additional scans for this study. Existing scans
106 were sourced through the online repository Morphosource (Project ID: 000642669), our previous
107 studies [8, 25] as well as completing additional scans. The source, museum identification, and the
108 scanning parameters for each specimen are provided in Supplementary Table 1. In total, we had brain
109 volume measurements and CT scans from 136 species, representing 58 families and 25 orders.
110 However, for four species, the volumes for either the telencephalon or cerebellum was unavailable –
111 two species from each region - reducing the total to 134 species for these brain regions.

112 *Endocast reconstruction and surface area data collection*

113 All endocast reconstruction and measurements were completed by AK. We imported the CT scans into
114 the image processing software Materialise Mimics (v.24.0; released in 2021 by Materialise NV) and
115 exported reconstructed skulls. Meshes of the inner surface of the brain cavity – the endocast – were
116 derived using the endomaker function from the Arothron package [59] in R [60] with the meshes
117 decimated to 20000 but otherwise using the base settings for all reconstructions. The meshes were
118 incomplete due to natural openings or damage to the skull, and often included excess material. To
119 complete the endocasts, these were imported into Geomagic Wrap (v.2021.2.2; released in 2023 by
120 3D Systems) to remove excess material and patch openings using the "flat" fill setting. Bumps and
121 crevices were also removed and subsequently patched with the "flat" fill along with the removal and
122 patching of nerves and blood vessels, following best practices as outlined by Balanoff, Bever [33]
123 (example in electronic supplementary material figure S1). As is to be expected, there was some
124 variation in the amount removed and patching needed for each specimen. However, efforts were
125 made to keep the reconstructions consistent and maintain the surface details of all the endocasts for
126 accuracy.

127 We defined the borders for the telencephalon and cerebellum by consulting previous studies which
128 partitioned endocasts for volume, surface area or landmark based measurements [4, 8, 21, 28, 61].
129 The posterior border of the telencephalon fossa was defined as the junction where it meets the
130 cerebellar fossa and continues ventrally through the crista tentorialis above the fossa tecti
131 mesenchephali. These borders then meet rostrally above the optic chiasma. For the cerebellum fossa,
132 the dorsal border was defined by the junction that meets the telencephalon fossa and continues along
133 the caudal border of the fossa tecti mesencephali on either side. This border continues as the crista
134 present at the ventral region of the cerebellum fossa, dorsal to the brainstem fossa, meeting in the
135 posterior region of the foramen magnum. We used the surface areas within these borders, which
136 encompass the visible imprints of both regions to estimate their sizes from the endocasts (Figures 1a,
137 b). We collected all measurements using Geomagic Wrap by following the borders outlined above. In
138 Figure 1c, we provide examples of these selections from each of the 25 clades in this study.

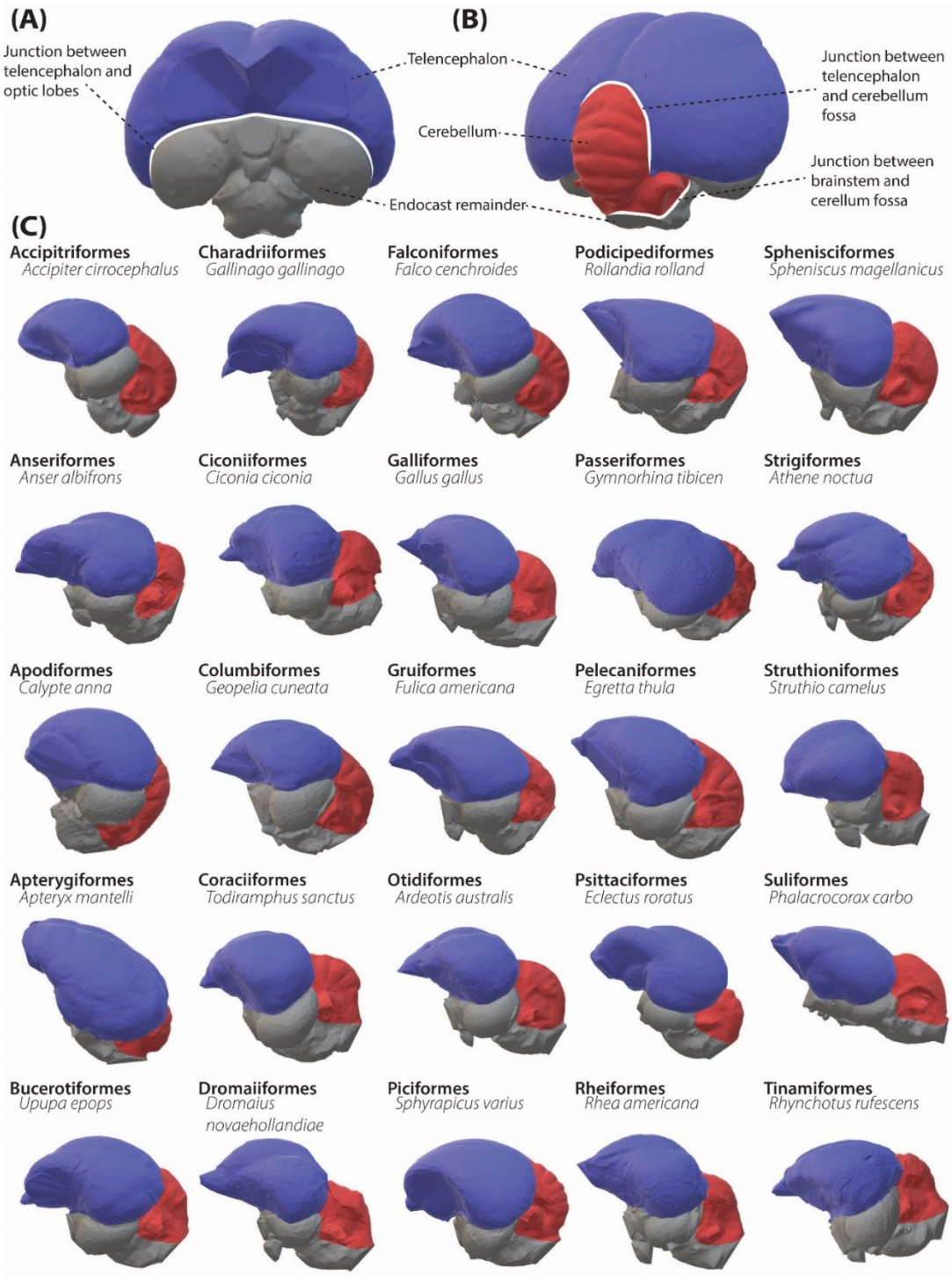

Figure 1. The endocast of a Eurasian treecreeper (*Certhia familiaris*) in rostral (A) and caudal views (B). Both images show osteological landmarks used to delineate the endocast telencephalon and cerebellum for measurements. The telencephalon is blue, the cerebellum is red, and the rest of the endocast is grey. (C) Endocasts of a representative species of each of the orders examined in this

144 study using the same colour coding as in A and B. Note that endocasts shown here are of reduced
145 resolution and are not to scale.

146 *Statistical analysis*

147 All data were natural log transformed for analyses. To assess if the absolute size of the endocast
148 surface areas is an appropriate proxy of the absolute size of their brain counterpart, we completed
149 ordinary least squares (OLS) regression analyses with brain region volume as predictor and endocast
150 surface area as response variables in R [60]. From these, we calculated confidence intervals (the
151 confidence of the fit), prediction intervals (the confidence with which an unknown specimen could be
152 given a value), and the line of best fit for each set of measurements: whole endocast, telencephalon
153 and cerebellum. We expected the endocast surface areas to scale isometrically with the brain volume,
154 with surface area scaling at two-thirds the volume (i.e., yielding slopes of 0.67). To test this, we
155 assessed the slope coefficients of the linear relationships and additionally used Wald tests in the *car*
156 package [62], which uses the model coefficients and coefficient-covariance matrix to determine if the
157 relationship significantly deviated from the isometric slope of 0.67 [63]. Note that the relationship
158 between brains and endocasts is not expected to be impacted by phylogenetic structure of the data.
159 For this reason, linear modelling was the preferred statistical procedure. However, phylogenetic
160 generalised least squares models were also computed using the *evomap* package [64] to assess if
161 phylogenetic relationships impact on the estimates of the slope [65].

162 As we have previously shown that the variation in voxel sizes of the CT scans may cause minor
163 discrepancies for endocast measurements [8] we tested if this may have had an artificial effect on
164 endocast size. We did this by calculating the residuals of OLS regression analyses using the whole
165 endocast surface area and whole brain volume as dependent variables and voxel size as the predictor
166 variable. We expected that if this factor does not influence the results that the residuals should show
167 a similar relationship to our comparisons of the endocast and brain measurements.

168 We also computed the relative size for both the telencephalon and cerebellum by scaling them with
169 the remainder of the brain as the dependent variable [66], both in the surface area (endocast-based)
170 data and the volume (histology-based) data. This was to confirm that the slopes of the scaling
171 relationships were comparable between the two data sets. Because phylogenetic relationships exert
172 a significant effect on the relative size of brain regions [43, 65, 67, 68], we used both linear modelling
173 and phylogenetic generalised least squares modelling to derive the slopes and intercepts.

174 We derived our phylogeny by pruning the family-level phylogeny by Stiller, Feng [69] and used
175 Mesquite [70] to place species on this tree using order specific phylogenetic studies [71-81]. We then
176 completed the PGLS regression analyses and calculated phylogenetic confidence intervals (CI) for each
177 of the regions against the remainder of either the endocast or brain using the *evomap* package [64].

178 **RESULTS**

179 Our comparisons of the surface area measurements for the whole endocast, telencephalon, and
180 cerebellum against their brain volume counterparts yielded highly significant associations (Figure 2;
181 Table 1) which are unlikely to be influenced by the voxel size (see electronic supplementary material,
182 figure S2). Furthermore, the resulting slopes indicate isometric relationships (Table 1) which are not
183 significantly different from the expected 0.67 according to the Wald test comparison (Table 1).While
184 this overall pattern is highly consistent, some species fell outside of the prediction intervals (PI) for
185 the whole sample, meaning that their surface area measurements were not expected given their
186 corresponding volumes. In total, nine species fell outside of the PIs for at least one of the regressions
187 with three outside of the PIs for all regressions: the satin bowerbird (*Ptilonorhynchus violaceus*;
188 Passeriformes), black-capped chickadee (*Poecile atricapillus*; Passeriformes), and the collared
189 sparrowhawk (*Accipiter cirrocephalus*; Accipitriformes) (Figure 2).

190 For the comparisons of the relative sizes of the telencephalon and cerebellum, the surface area for
191 these regions regressed against the endocast remainder yielded similar slopes to that of the region
192 volume regressed against the brain remainder, for both the OLS and PGLS (Figure 3; Table 2). Parrots
193 (Psittaciformes) appear to deviate more from the regression lines in Figure 3 for both regions. This is
194 because parrots have relatively large telencephala and small cerebella compared with other species
195 [43]. The surface area measurements show a somewhat larger deviation for the telencephalon, which
196 could arise from the relationship between surface area and volume or that the optic lobes are smaller
197 in parrots [43, 82], allowing the telencephalon to spread out more. One species, the Kākāpō (*Strigops*
198 *habroptilus*), is outside of the PGLS confidence interval for the expected range of the telencephalon
199 surface area scaled against the endocast remainder surface area (Figure 3a). This species is a uniquely
200 nocturnal and flightless parrot that is neuroanatomically distinct within its clade [54] which may then
201 result in an atypical relationship between endocast and brain measurements. Overall, these results

202 indicate that the scaling relationship for both brain regions is similar when measured from endocast

203 surface areas and brain volumes.

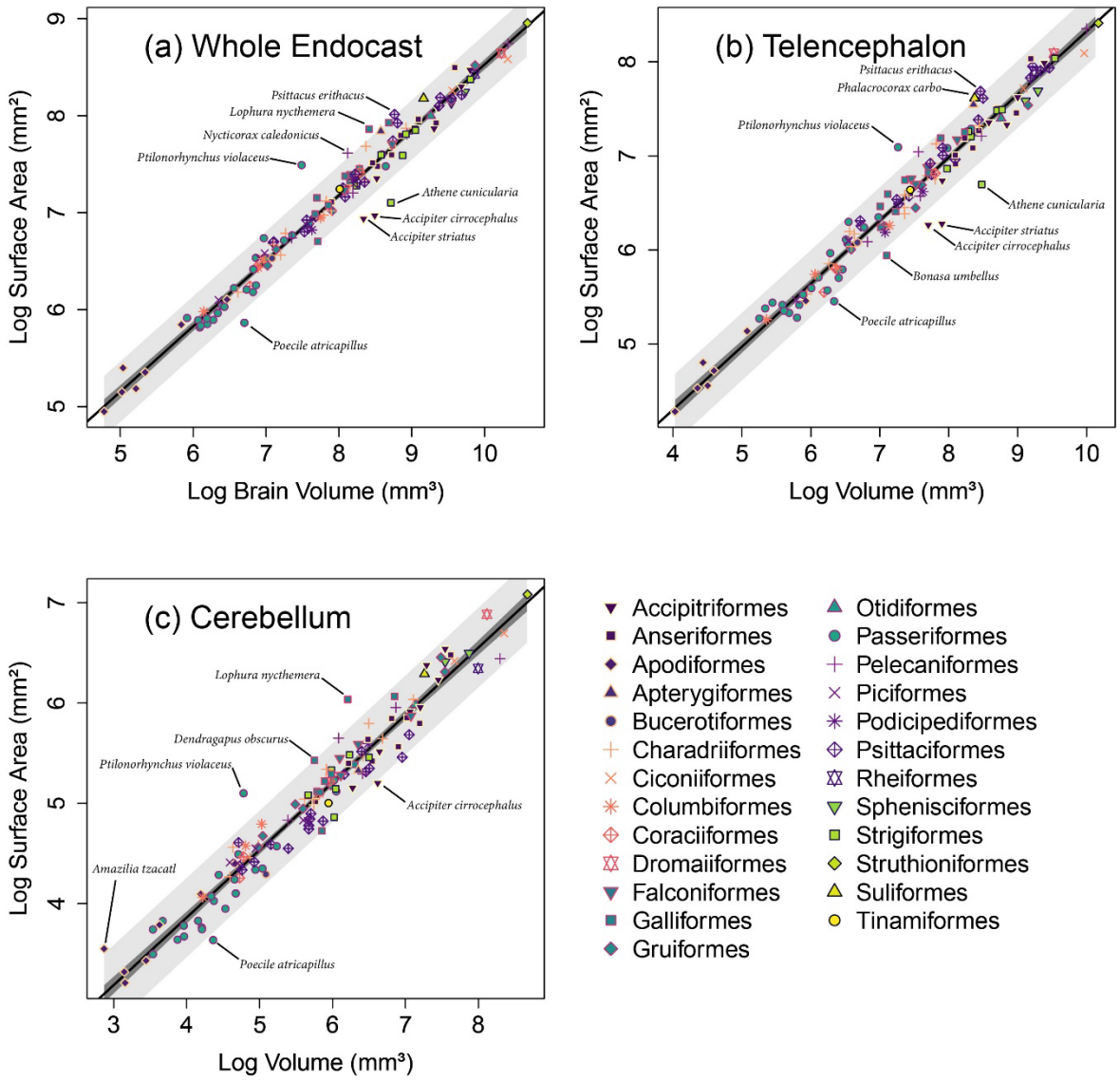

204

205 **Figure 2.** Log transformed measurements of the (a) whole endocast, (b) telencephalon, and (c)

206 cerebellum surface areas measured from endocasts regressed against their brain volume counterparts

207 for 136 species of birds. The orders from this data are represented by unique combinations of colours

208 with point shapes. The black line represents the ordinary least-squares linear model regression; dark

209 grey area represents 95% confidence intervals; light grey area represents 95% prediction intervals.

210 **Table 1.** Results from ordinary least squares (OLS) regression analyses and Wald tests. OLS results
211 show the significant (p=<0.05) relationships between the endocast surface area measurements and
212 the brain volume measurements. Wald test results show that slopes do not significantly (*p*=>0.05)
213 differ from the expected isometric relationship between surface area and volume measurements
214 (0.67).

Dependent	Predictor	*df*	F-statistic	*p*-value	*y* intercept	R^2	Slope	Wald test *p*-value
log Endo. SA	log Brain VOL	134	3969	<0.01	1.78	0.97	0.68	0.64
log Tele. SA	log Tele. VOL	132	2954	<0.01	1.62	0.96	0.67	0.99
log Cere. SA	log Cere. VOL	132	2324	<0.01	1.17	0.95	0.67	0.84

215 Abbreviations: SA, surface area; Vol., volume; Endo., endocast; Tele., telencephalon; Cere.,
216 cerebellum.

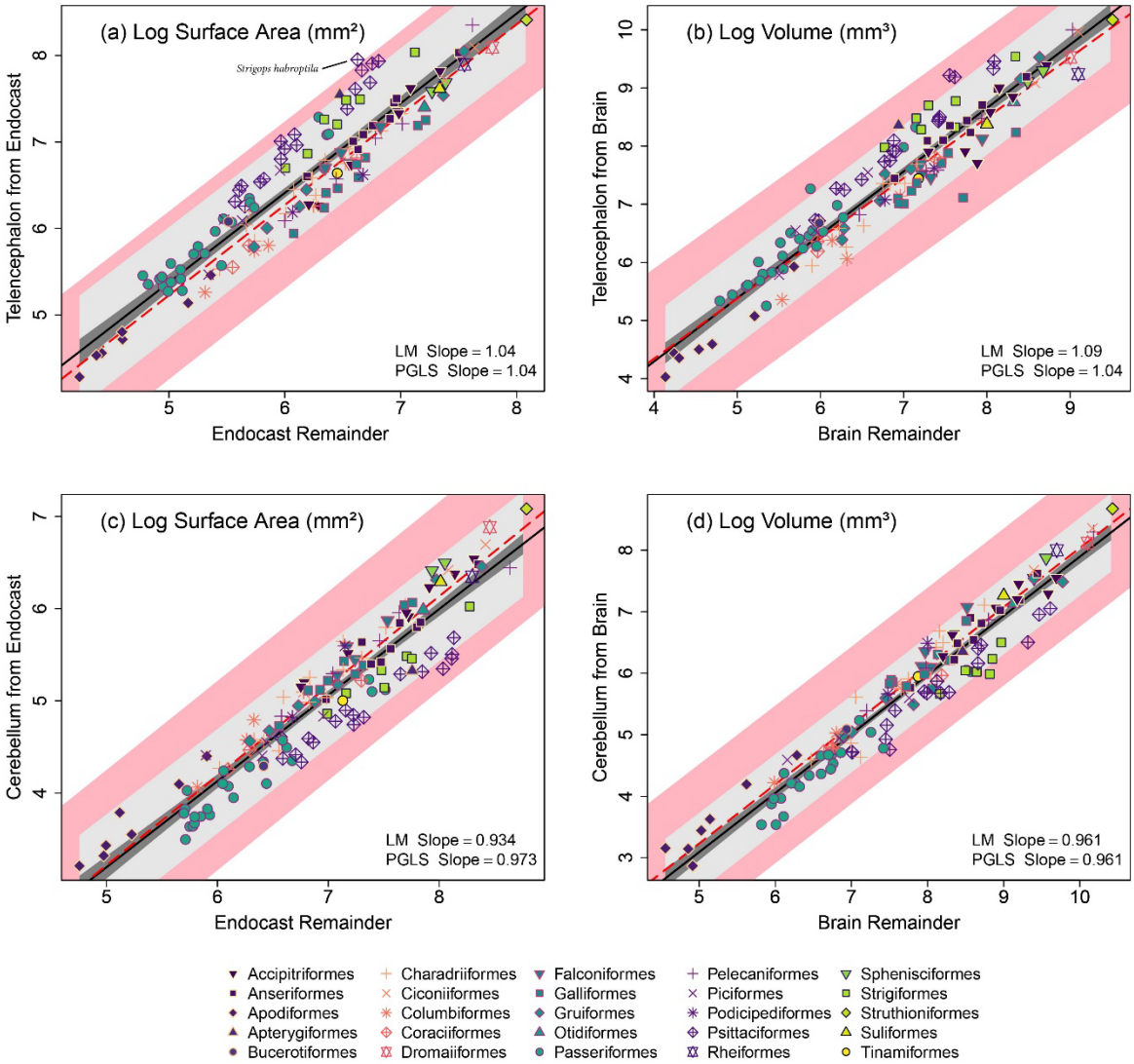

Figure 3. Log transformed measurements comparing the scaling relationships of the telencephalon for (a) the surface area against endocast remainder, and (b) the volume against brain remainder, as well as the cerebellum for (c) the surface area against endocast remainder, and (d) the volume against brain remainder for 136 species of birds. The orders from this data are represented by unique combinations of colours with point shapes. Ordinary least squares regression (LM slope) is shown by the black line; dark grey for the 95% confidence intervals; light grey for the 95% prediction intervals. Phylogenetic generalised least squares (PGLS) regression shown by the dashed red line; pink area shows the 95% confidence intervals of the PGLS.

226 **Table 2.** Results from phylogenetic generalised least squares (PGLS) regression models used to
227 compare the scaling relationship of endocast surface area and brain volume measurements of the
228 telencephalon and cerebellum.

Dependent	Predictor	*df*	*t*-value	*p*-value	*y* intercept	Slope
Tele. SA.	Endo. Remainder	134	32.2	<0.01	0	1.04
Tele. VOL	Brain remainder	134	28.97	<0.01	0.2	1.04
Cere. SA	Endo. Remainder	134	29.35	<0.01	-1.65	0.97
Cere. VOL	Brain remainder	134	33.48	<0.01	-1.57	0.96

229 Abbreviations: SA, surface area; Vol., volume; Endo., endocast; Tele., telencephalon; Cere.,
230 cerebellum.

231

232 **DISCUSSION**

233 Our results reveal that avian endocast surface areas for the whole endocast, the telencephalon, and
234 the cerebellum exhibit tight isometric relationships with the volume of their brain counterparts. This
235 result is in spite of a sample size of one individual per species for the endocast measurements and a
236 reliance on different individuals for the endocast and brain measurements, both of which could have
237 reduced the strength of the association between the two datasets [31]. By including a broad range of
238 species, our validation supports the use of endocast measurements for these regions in future studies,
239 while also supporting the conclusions from previous studies which relied on such measurements [8,
240 9, 25, 36, 37, 83, 84]. This result is particularly beneficial for studies on rare species [8, 25], and
241 palaeontological specimens [9, 85] for which brain measurements are not attainable.

We also found that the relative sizes for both the telencephalon and cerebellum regions are consistent between the endocast surface areas and the soft tissue brain volumes, supporting their use in comparisons of brain composition [43]. This is in spite of the absence of the entire anterior lobe of the cerebellum in endocasts which is generally hidden from external view by the telencephalon, and the cerebellar surface often obscured by the occipital sinus [3, 32, 86, 87]. For other endocast validation research, such as that of the optic lobes and wulst [28], the regions are typically clearly defined and largely unobscured. Nonetheless, our findings strongly suggest that the portion of the cerebellum visible in endocasts is sufficient for estimating its relative volume.

While there is a strong brain–endocast association despite our reliance on different individuals, some species showed disparities between specimens, likely due to intraspecific variation in brain size and composition arising from sexual dimorphism [88-90] or subspecific, clinal, and other regional variation [91]. In fact, in a previous study, we found substantial skull and endocast size differences for two collared sparrowhawk specimens, likely due to sexual dimorphism [25]. Within this study, we suspect variation from sexual dimorphism in hawks [88, 90], and pheasants [56, 92],and regional variation for the bowerbird [89], chickadee [93], burrowing owl [94] and cormorant [95]. Furthermore, as variation occurred when comparing volumes and surface areas directly to one another but did not appear to be present in the analyses of relative brain region size we suspect this variation stems from using different specimens for both datasets. While variation is expected, this raises concerns regarding the sample size needed to represent a species in comparative studies, particularly of narrow taxonomic scope. We nevertheless note the high correspondence between the brain and endocast datasets, suggesting that these measurements can generally be used with small sample sizes.

The telencephalon and cerebellum make up the majority of the brain and endocast surface, making their inclusion necessary for studies on brain composition [43]. By using known brain–behaviour associations, such as the telencephalon size with cognitive abilities [36, 40, 96], and the cerebellum with flight abilities [37, 38, 42], some aspects of ecology and behaviours may be inferred from these

regions [40, 46, 97-99]. Furthermore, even though some behaviourally relevant brain regions (such as the hippocampus [100]) will always remain hidden within the brain, holistic approaches to endocast comparisons can improve the accuracy of inferences by accounting for the influences that changes in brain regions sizes can have on one another [14, 43, 99, 101]. For example, the relative size of the telencephalon in owls is comparable with that of parrots [96], but this is largely due to their hypertrophied wulst in relation to vision [43] and not the regions of the telencephalon associated with cognition [102].

Overall, this study has confirmed the strong relationships between the surface areas of endocasts and brain volumes in birds for absolute and relative size, both wholly and when divided into the telencephalon and cerebellum regions. This result is in concordance with other endocast validations [28, 31], and we suggest that further expanding the use of avian endocasts is plausible. However, these methods remain speculative beyond the crown group Aves, such as for non-avian dinosaurs [2, 4, 29]. Outside of validating bird endocasts, comparisons with other living archosaurs, the crocodilians, may assist with resolving the brain–endocast correspondence [2] and provide further evidence for the strengths and limitations of these methods [4, 30]. With the increased accessibility that CT scanning and associated digital reconstruction methods present [1, 10, 103], expanding and refining endocast uses has the potential to shed light on the lives of extinct species and further resolve our understanding of vertebrate brain evolution.

REFERENCES

1. Degrange, F.J., et al., *Anatomy and Evolution of Avian Brain and Senses: What Endocasts Can Tell Us*, in *Paleoneurology of Amniotes : New Directions in the Study of Fossil Endocasts*, M.T. Dozo, et al., Editors. 2023, Springer International Publishing: Cham. p. 333-364.
2. Clement, A.M., et al., *Brain Reconstruction Across the Fish-Tetrapod Transition; Insights From Modern Amphibians.* Frontiers in Ecology and Evolution, 2021. **9**.
3. Balanoff, A. and G.S. Bever, *The Role of Endocasts in the Study of Brain Evolution*. 2017. p. 223-241.
4. Watanabe, A., et al., *Are endocasts good proxies for brain size and shape in archosaurs throughout ontogeny?* Journal of Anatomy, 2019. **234**(3): p. 291-305.
5. Clement, A.M., et al., *Morphometric analysis of lungfish endocasts elucidates early dipnoan palaeoneurological evolution.* eLife, 2022. **11**: p. e73461.
6. Weisbecker, V., et al., *Global elongation and high shape flexibility as an evolutionary hypothesis of accommodating mammalian brains into skulls.* Evolution, 2021. **75**(3): p. 625-640.
7. Kubo, D., et al., *Accuracy and precision of CT-based endocranial capacity estimations: a comparison with the conventional millet seed method and application to the Minatogawa 1 skull.* Anthropological Science, 2008. **116**(1): p. 77-85.
8. Iwaniuk, A.N., et al., *The endocast of the Night Parrot (Pezoporus occidentalis) reveals insights into its sensory ecology and the evolution of nocturnality in birds.* Scientific Reports, 2020. **10**(1): p. 9258.
9. Torres, C.R. and J.A. Clarke, *Nocturnal giants: evolution of the sensory ecology in elephant birds and other palaeognaths inferred from digital brain reconstructions.* Proceedings. Biological sciences, 2018. **285**(1890).
10. Knoll, F. and S. Kawabe, *Avian palaeoneurology: Reflections on the eve of its 200th anniversary.* Journal of Anatomy, 2020. **236**(6): p. 965-979.
11. Heingård, M., et al., *New Remains of Scandiavis mikkelseni Inform Avian Phylogenetic Relationships and Brain Evolution.* Diversity, 2021. **13**(12).
12. Walsh, S.A. and M.A. Knoll, *Directions in palaeoneurology.* Special Papers in Palaeontology, 2011. **86**(1228): p. 263-279.
13. Buchholtz, E.A. and E.-A. Seyfarth, *The Study of "Fossil Brains": Tilly Edinger (1897–1967) and the Beginnings of Paleoneurology.* BioScience, 2001. **51**(8): p. 674-682.
14. Ksepka, D.T., et al., *Tempo and Pattern of Avian Brain Size Evolution.* Curr Biol, 2020. **30**(11): p. 2026-2036.e3.
15. Beyrand, V., et al., *Multiphase progenetic development shaped the brain of flying archosaurs.* Scientific Reports, 2019. **9**(1): p. 10807.
16. Allemand, R., et al., *Comparative morphology of snake (Squamata) endocasts: evidence of phylogenetic and ecological signals.* Journal of Anatomy, 2017. **231**(6): p. 849-868.
17. Todorov, O.S., et al., *Down a Rabbit Hole: Burrowing Behaviour and Larger Home Ranges are Related to Larger Brains in Leporids.* Journal of Mammalian Evolution, 2022. **29**(4): p. 957-967.
18. Marino, L., et al., *Reconstructing cetacean brain evolution using computed tomography.* The anatomical record. Part B, New anatomist, 2003. **272B**(1): p. 107-117.
19. Montgomery, S.H., et al., *Reconstructing the ups and downs of primate brain evolution: implications for adaptive hypotheses and Homo floresiensis.* BMC Biology, 2010. **8**(1): p. 9.
20. Carril, J., et al., *Comparative brain morphology of Neotropical parrots (Aves, Psittaciformes) inferred from virtual 3D endocasts.* Journal of Anatomy, 2016. **229**(2): p. 239-251.
21. Balanoff, A.M., J.B. Smaers, and A.H. Turner, *Brain modularity across the theropod–bird transition: testing the influence of flight on neuroanatomical variation.* Journal of anatomy, 2016. **229**(2): p. 204-214.

22. Edinger, T., *Paleoneurology 1804-1966 : an annotated bibliography*. 1st 1975. ed. Advances in Anatomy, Embryology and Cell Biology, 49. 1975, Berlin ;: Springer-Verlag.
23. Edinger, T., *The brain of Pterodactylus.* American journal of science: devoted to the geological sciences and to related fields, 1941. **239**(9): p. 665.
24. Sakai, S.T., et al., *Big Cat Coalitions: A Comparative Analysis of Regional Brain Volumes in Felidae.* Frontiers in Neuroanatomy, 2016. **10**.
25. Keirnan, A., et al., *Not like night and day: the nocturnal letter-winged kite does not differ from diurnal congeners in orbit or endocast morphology.* Royal Society Open Science, 2022. **9**(5): p. 220135.
26. Jerison, H.J., *Evolution of the Brain and Intelligence.* Current Anthropology, 1975. **16**(3): p. 403-426.
27. Sakai, S.T., et al., *Virtual endocasts: an application of computed tomography in the study of brain variation among hyenas.* Annals of the New York Academy of Sciences, 2011. **1225**(S1): p. E160-E170.
28. Early, C.M., et al., *Endocast structures are reliable proxies for the sizes of corresponding regions of the brain in extant birds.* Journal of Anatomy, 2020. **237**(6): p. 1162-1176.
29. Morhardt, A.C., R.C. Ridgely, and L.M. Witmer. *From endocast to brain: assessing brain size and structure in extinct archosaurs using gross anatomical brain region approximation (GABRA)*. in *Journal of Vertebrate Paleontology*. 2012. TAYLOR & FRANCIS INC 325 CHESTNUT ST, SUITE 800, PHILADELPHIA, PA 19106 USA.
30. Jirak, D. and J. Janacek, *Volume of the crocodilian brain and endocast during ontogeny.* PLOS ONE, 2017. **12**(6): p. e0178491.
31. Iwaniuk, A. and J. Nelson, *Can endocranial volume be used as an estimate of brain size in birds? Can J Zool.* Canadian Journal of Zoology, 2002. **80**: p. 16-23.
32. Witmer, L.M., et al., *Using CT to Peer into the Past: 3D Visualization of the Brain and Ear Regions of Birds, Crocodiles, and Nonavian Dinosaurs*, in *Anatomical Imaging: Towards a New Morphology*, H. Endo and R. Frey, Editors. 2008, Springer Japan: Tokyo. p. 67-87.
33. Balanoff, A.M., et al., *Best practices for digitally constructing endocranial casts: examples from birds and their dinosaurian relatives.* Journal of Anatomy, 2016. **229**(2): p. 173-190.
34. Smaers, J.B., et al., *The evolution of mammalian brain size.* Science Advances. **7**(18): p. eabe2101.
35. Weisbecker, V. and A. Goswami, *Brain size, life history, and metabolism at the marsupial/placental dichotomy.* Proceedings of the National Academy of Sciences, 2010. **107**(37): p. 16216-16221.
36. Walsh, S.A. and F. Knoll, *The Evolution of Avian Intelligence and Sensory Capabilities: The Fossil Evidence*. 2017, Tokyo: Springer Japan: Tokyo. p. 59-69.
37. Balanoff, A.M., et al., *Evolutionary origins of the avian brain.* Nature, 2013. **501**(7465): p. 93-96.
38. Witmer, L.M., et al., *Neuroanatomy of flying reptiles and implications for flight, posture and behaviour.* Nature, 2003. **425**(6961): p. 950-953.
39. Striedter, G.F. and R.G. Northcutt, *Brains through time: a natural history of vertebrates*. 2019: Oxford University Press.
40. Lefebvre, L., et al., *Feeding innovations and forebrain size in birds.* Animal behaviour, 1997. **53**(3): p. 549-560.
41. Cunha, F., et al., *A quantitative analysis of cerebellar anatomy in birds.* Brain Structure and Function, 2021. **226**(8): p. 2561-2583.
42. Iwaniuk, A.N., P.L. Hurd, and D.R.W. Wylie, *Comparative Morphology of the Avian Cerebellum: II. Size of Folia.* Brain, behavior and evolution, 2007. **69**(3): p. 196-219.
43. Iwaniuk, A.N. and P.L. Hurd, *The evolution of cerebrotypes in birds.* Brain, Behavior and Evolution, 2005. **65**(4): p. 215-230.

44. Sol, D., et al., *Evolutionary Divergence in Brain Size between Migratory and Resident Birds.* PLOS ONE, 2010. **5**(3): p. e9617.
45. Sol, D., L. Lefebvre, and J.D. Rodríguez-Teijeiro, *Brain size, innovative propensity and migratory behaviour in temperate Palaearctic birds.* Proceedings of the Royal Society B: Biological Sciences, 2005. **272**(1571): p. 1433-1441.
46. Barros da Cunha, F., *Allometric Relationships and the Evolution of the Avian Brain*. 2021, ProQuest Dissertations Publishing.
47. Iwaniuk, A.N. and J.E. Nelson, *Developmental differences are correlated with relative brain size in birds: a comparative analysis.* Canadian journal of zoology, 2003. **81**(12): p. 1913-1928.
48. Portmann, A., *Etudes sur la cérébralisation des oiseaux. II. Les indices intra-cérébraux.* Alauda, 1947. **15**: p. 1-15.
49. Kalisińska, E., *Anseriform brain and its parts versus taxonomic and ecological categories.* Brain, Behavior and Evolution, 2005. **65**(4): p. 244-261.
50. Corfield, J.R., et al., *Morphometric Analysis of Telencephalic Structure in a Variety of Neognath and Paleognath Bird Species Reveals Regional Differences Associated with Specific Behavioral Traits.* Brain, Behavior and Evolution, 2012. **80**(3): p. 181-195.
51. Alama, S. and N. Bee-dee-Speroni, *índices cerebrales y composición cuantitativa encefálica en Athene cunicularia y Tyto alba (Strigiformes: Strigidae y Tytonidae).* Facena, 1992. **9**: p. 19-37.
52. Boire, D. and G.J.J.o.B.R. Baron, *Allometric comparison of brain and main brain subdivisions in birds.* 1994. **35**(1): p. 49-66.
53. Carezzano, F. and N. Bee de Speroni, *Composicion volumetrica encefalica e indices cerebrales en tres aves de ambiente acuatico (Ardeidae, Podicipedidae, Rallidae).* Facena, 1995. **11**: p. 75-83.
54. Corfield, J.R., et al., *Anatomical Specializations for Nocturnality in a Critically Endangered Parrot, the Kakapo (Strigops habroptilus) (Visual System of the Kakapo).* PLoS ONE, 2011. **6**(8): p. e22945.
55. Day, L.B., D.A. Westcott, and D.H. Olster, *Evolution of bower complexity and cerebellum size in bowerbirds.* Brain behavior and evolution, 2005. **66**(1): p. 62-72.
56. Krilow, J.M. and A.N. Iwaniuk, *Seasonal Variation in Forebrain Region Sizes in Male Ruffed Grouse (Bonasa umbellus).* Brain, Behavior and Evolution, 2015. **85**(3): p. 189-202.
57. Iwaniuk, A.N., *The importance of scientific collecting and natural history museums for comparative neuroanatomy.* Annals of the New York Academy of Sciences, 2011. **1225**(S1): p. E1-E19.
58. Keirnan, A.R., et al., *Avian telencephalon and cerebellum volumes can be accurately estimated from digital brain endocasts* 2024.
59. Profico, A., et al., *Endomaker, a new algorithm for fully automatic extraction of cranial endocasts and the calculation of their volumes.* American Journal of Physical Anthropology, 2020. **172**(3): p. 511-515.
60. R Core Team, *R: A language and environment for statistical computing. R Foundation for Statistical Computing, Vienna, Austria.* 2021, R Foundation for Statistical Computing,.
61. Kawabe, S., et al., *Variation in avian brain shape: relationship with size and orbital shape.* J Anat, 2013. **223**(5): p. 495-508.
62. Fox, J. and S. Weisberg, *An R companion to applied regression*. 2018: Sage publications.
63. Goldman, C.A., et al., *Principles of allometry.* Tested studies for laboratory teaching, 1990. **11**: p. 43-72.
64. Smaers, J. and C. Mongle, *evomap: R package for the evolutionary mapping of continuous traits.* GitHub (https://github. com/JeroenSmaers/evomap), 2014.

65. Garland, T., Jr. and A.R. Ives, *Using the Past to Predict the Present: Confidence Intervals for Regression Equations in Phylogenetic Comparative Methods.* Am Nat, 2000. **155**(3): p. 346-364.
66. Deacon, T.W., *Fallacies of progression in theories of brain-size evolution.* International Journal of Primatology, 1990. **11**(3): p. 193-236.
67. Garland, T., Jr., A.F. Bennett, and E.L. Rezende, *Phylogenetic approaches in comparative physiology.* Journal of Experimental Biology, 2005. **208**(16): p. 3015-3035.
68. Corfield, J.R., et al., *Diversity in olfactory bulb size in birds reflects allometry, ecology, and phylogeny.* Front Neuroanat, 2015. **9**: p. 102.
69. Stiller, J., et al., *Complexity of avian evolution revealed by family-level genomes.* Nature, 2024.
70. Maddison, W.P. and D.R. Maddison, *Mesquite: a modular system for evolutionary analysis. Version 3.81*. 2023.
71. Fuchs, J., J.A. Johnson, and D.P. Mindell, *Rapid diversification of falcons (Aves: Falconidae) due to expansion of open habitats in the Late Miocene.* Molecular Phylogenetics and Evolution, 2015. **82**: p. 166-182.
72. Prum, R.O., et al., *A comprehensive phylogeny of birds (Aves) using targeted next-generation DNA sequencing.* Nature, 2015. **526**(7574): p. 569-573.
73. Andersen, M., et al., *A phylogeny of kingfishers reveals an Indomalayan origin and elevated rates of diversification on oceanic islands.* Journal of Biogeography, 2017. **45**.
74. Shakya, S.B., et al., *Tapping the woodpecker tree for evolutionary insight.* Molecular Phylogenetics and Evolution, 2017. **116**: p. 182-191.
75. Garcia-R, J.C., et al. *Phylogenomic Reconstruction Sheds Light on New Relationships and Timescale of Rails (Aves: Rallidae) Evolution*. Diversity, 2020. **12**, DOI: 10.3390/d12020070.
76. Kimball, R.T., P.A. Hosner, and E.L. Braun, *A phylogenomic supermatrix of Galliformes (Landfowl) reveals biased branch lengths.* Mol Phylogenet Evol, 2021. **158**: p. 107091.
77. Wink, M. and H. Sauer-Gurth, *Molecular taxonomy and systematics of owls (Strigiformes)—An update.* Airo, 2021. **29**: p. 487-500.
78. Černý, D. and R. Natale, *Comprehensive taxon sampling and vetted fossils help clarify the time tree of shorebirds (Aves, Charadriiformes).* Molecular Phylogenetics and Evolution, 2022. **177**: p. 107620.
79. Hruska, J.P., et al., *Ultraconserved elements resolve the phylogeny and corroborate patterns of molecular rate variation in herons (Aves: Ardeidae).* Ornithology, 2023. **140**(2): p. ukad005.
80. Catanach, T.A., M.R. Halley, and S. Pirro, *Enigmas no longer: using ultraconserved elements to place several unusual hawk taxa and address the non-monophyly of the genus Accipiter (Accipitriformes: Accipitridae).* Biological journal of the Linnean Society, 2024.
81. Smith, B.T., et al., *Phylogenomic Analysis of the Parrots of the World Distinguishes Artifactual from Biological Sources of Gene Tree Discordance.* Systematic Biology, 2023. **72**(1): p. 228-241.
82. Iwaniuk, A.N., et al., *Allometric Scaling of the Tectofugal Pathway in Birds.* Brain, Behavior and Evolution, 2010. **75**(2): p. 122-137.
83. Early, C.M., R.C. Ridgely, and L.M. Witmer, *Beyond endocasts: Using predicted brain-structure volumes of extinct birds to assess neuroanatomical and behavioral inferences.* Diversity, 2020. **12**(1).
84. Milner, A.C. and S.A. Walsh, *Avian brain evolution: new data from Palaeogene birds (Lower Eocene) from England.* Zoological journal of the Linnean Society, 2009. **155**(1): p. 198-219.
85. Smith, N.A. and J.A. Clarke, *Endocranial Anatomy of the Charadriiformes: Sensory System Variation and the Evolution of Wing-Propelled Diving.* PLOS ONE, 2012. **7**(11): p. e49584.

86. Ksepka, D.T., et al., *Evolution of the brain and sensory organs in Sphenisciformes: new data from the stem penguin Paraptenodytes antarcticus: PENGUIN BRAIN EVOLUTION.* Zoological journal of the Linnean Society, 2012: p. no-no.
87. Walsh, S.A., et al., *Avian Cerebellar Floccular Fossa Size Is Not a Proxy for Flying Ability in Birds.* PloS one, 2013. **8**(6): p. e67176-e67176.
88. Debus, S.J.S., *Birds of prey of Australia: a field guide*. 2nd ed. ed, ed. J.N. Davies and A. BirdLife. 2012, Collingwood, Vic.: Collingwood, Vic. : CSIRO Publishing in association with Birdlife Australia.
89. Menkhorst, P., et al., *The Australian bird guide*. 2017: Csiro Publishing Melbourne.
90. Dunne, P. and K.T. Karlson, *Birds of Prey: Hawks, Eagles, Falcons, and Vultures of North America*. 2017: Houghton Mifflin Harcourt.
91. Baladrón, A.V., et al., *Body size and sexual dimorphism in the southernmost subspecies of the Burrowing Owl (Athene cunicularia cunicularia).* Journal of Raptor Research, 2015. **49**(4): p. 479-485.
92. McGowan, P.J.K. and G.M. Kirwan. *Silver Pheasant (Lophura nycthemera), version 1.0. In Birds of the World (J. del Hoyo, A. Elliott, J. Sargatal, D. A. Christie, and E. de Juana, Editors)*. 2020 [cited 2024.
93. Roth, T.C. and V.V. Pravosudov, *Hippocampal volumes and neuron numbers increase along a gradient of environmental harshness: a large-scale comparison.* Proc Biol Sci, 2009. **276**(1656): p. 401-5.
94. Poulin, R.G., et al. *Burrowing Owl (Athene cunicularia), version 1.0. In Birds of the World (A. F. Poole, Editor)*. 2020.
95. Hatch, J.J., et al. *Great Cormorant (Phalacrocorax carbo), version 1.0. In Birds of the World (S. M. Billerman, Editor)*. 2020 [cited 2024.
96. Iwaniuk, A.N., K.M. Dean, and J.E. Nelson, *Interspecific Allometry of the Brain and Brain Regions in Parrots (Psittaciformes): Comparisons with Other Birds and Primates.* Brain Behav Evol, 2004. **65**(1): p. 40-59.
97. Burish, M.J., H.Y. Kueh, and S.S.H. Wang, *Brain Architecture and Social Complexity in Modern and Ancient Birds.* Brain, behavior and evolution, 2004. **63**(2): p. 107-124.
98. Lefebvre, L., et al., *Feeding Innovations and Forebrain Size in Australasian Birds.* Behaviour, 1998. **135**(8/9): p. 1077-1097.
99. Iwaniuk, A.N., K.M. Dean, and J.E. Nelson, *A mosaic pattern characterizes the evolution of the avian brain.* Proceedings of the Royal Society B: Biological Sciences, 2004. **271**(Suppl 4): p. S148-S151.
100. Todorov, O.S., et al., *Primate hippocampus size and organization are predicted by sociality but not diet.* Proceedings of the Royal Society B: Biological Sciences, 2019. **286**(1914): p. 20191712.
101. Carlisle, A., et al., *Testing hypotheses of developmental constraints on mammalian brain partition evolution, using marsupials.* Scientific Reports, 2017. **7**(1): p. 4241.
102. Sayol, F., et al., *Environmental variation and the evolution of large brains in birds.* Nature Communications, 2016. **7**(1): p. 13971.
103. Davies, T.G., et al., *Open data and digital morphology.* Proceedings of the Royal Society B: Biological Sciences, 2017. **284**(1852): p. 20170194.